Colloidal quantum-dot LEDs with a solution-processed copper oxide (CuO) hole injection layer

CrossMark

Tao Ding [a], Xuyong Yang [a], Linyi Bai [b], Yongbiao Zhao [a], Kah Ee Fong [a], Ning Wang [a], Hilmi Volkan Demir [a,b,*], Xiao Wei Sun [a,*]

[a] Luminous! Center of Excellence for Semiconductor Lighting and Displays, School of Electrical and Electronic Engineering, Nanyang Technological University, 50 Nanyang Avenue, Singapore 639798, Singapore
[b] Division of Physics and Applied Physics, School of Physical and Mathematical Sciences, Nanyang Technological University, 21 Nanyang Link, Singapore 637371, Singapore

ARTICLE INFO

ABSTRACT

Solution-processed copper oxide (CuO) thin films are introduced as a hole injection layer (HIL) for quantum dot-based light-emitting diodes (QD-LEDs). AFM, XPS and UPS measurements are utilized for the characterization of the thermally-annealed CuO films. The optimized CuO-based QD-LEDs exhibited an external quantum efficiency (EQE) of 5.37% with a maximum brightness over 70,000 cd/m^2. The key parameters including the current efficiency and power efficiency of CuO-based QD-LEDs are comparable to the commonly-used PEDOT:PSS-based QD-LEDs using the same structure, further demonstrating that CuO is an effective hole injection layer for QD-LED applications.

© 2015 Elsevier B.V. All rights reserved.

1. Introduction

Due to their tunable wavelength across the whole visible range and narrow full-width-at-half-maximum (FWHM) [1–3], quantum dot light-emitting diodes (QD-LEDs) have been regarded as a strong candidate for the next-generation solid state lighting and displays [2–5]. Since the first demonstration two decades ago [6], some key device parameters, including the external quantum efficiency (EQE), brightness, current efficiency of QD-LEDs have improved significantly as a result of the optimization of the device architecture and advancement of the fabrication techniques [7–10], the choices of proper materials for charge injection and transportation [5,11–13] and the structural variation of the QDs themselves [14–17]. Recent reports have demonstrated that some features of QD-LEDs can be comparable, or even superior to other high-performance polymer/small-molecule OLEDs [18,19], further proving their competence for an important role in optoelectronic area.

Among the reported QD-LEDs with high efficiency, poly (3,4-ethylenedioxythiophene) polystyrene sulfonate (PEDOT:PSS) is frequently used as buffer layer atop of the indium tin oxide (ITO) electrode to facilitate the carrier injection [2,18,20]. However, the PEDOT:PSS layer tends to etch the ITO electrode by acidic corrosion, thus resulting in the device instability and degradation with time [21]. Also, compared with inorganic materials, PEDOT:PSS is chemically more unstable, which further cast itself in doubt for long term use in QD-LEDs [11]. Therefore, alternative inorganic hole transporting materials for substituting PEDOT:PSS have attracted significant interest. For example, Caruge et al. reported an inorganic/organic QD-LED by applying nickel oxide as the hole transporting layer [11]. However, the external quantum efficiency was relatively low (0.18%) because of the rough interface between NiO and ITO due to RF sputtering technique. Recently, zinc-, molybdenum-, tungsten-, copper-, rhenium-, or vanadium-oxides have been demonstrated as charge transport layers in optoelectronic devices to improve the device efficiency and stability [21–25]. For electron injection, in the all reported QD-LEDs with high efficiencies, zinc oxide (ZnO) nanoparticles are generally used as electron transport layers because of their high electron mobility as well as efficient electron injection into the active layer [2,19]. For hole injection, our group has reported using tungsten oxide (WO$_3$) nanoparticles in QD-LEDs as hole injection layers [26,27]. Although the performance was limited, our work successfully demonstrated the possibility of applying metal oxide materials as the hole injection layer (HIL) in QD-LEDs. Moving forward, here

---

in this work, we shall report employing copper oxide (CuO) instead of PEDOT:PSS as a hole injection layer for high performance QD-LEDs based on the fact that this inorganic material has been successfully demonstrated as the qualified hole transport layer for polymer solar cells because its workfunction is comparable with the highest occupied molecular orbital (HOMO) energy level of PEDOT:PSS [28,29].

The measured valence band maximum (VBM) of CuO is around 5.5 eV, which is close to the HOMO level of PEDOT:PSS. The copper oxide layer on an ITO electrode is prepared by a facile solution process from copper acetate solution and thermally annealed inside the nitrogen-filled glovebox. We demonstrated that CuO thin films act as a qualified HIL in QD-LEDs by presenting a peak EQE over 5%, a maximum luminance over 70,000 cd/m^2, and a peak current efficiency of 21.3 cd/A, which are comparative or better compared to those of QD-LEDs based on organic HIL counterpart. To the best of our knowledge, no literature using CuO as HIL in QD-LED has been reported yet. And the performances of our fabricated devices are among the highest performance QD-LEDs using metal oxide as the hole injection layers by far.

2. Experimental details

2.1. Materials

2.1.1. Synthesis of QDs and CuO solution

Green emitting CdSe@ZnS QDs with chemical composition gradients were prepared by a modified one-pot synthesis as reported in the literature [30]. Briefly, 0.14 mmol of Cd acetate, 3.41 mmol of zinc oxide and 7 ml of OA were mixed in a 50 ml four-neck flask. The mixture was heated to 100 °C with degassing under 0.03 mTorr pressure for 20 min. Then, 15 ml of ODE was added into the reactor, and the whole mixture was degassed again to 100 °C. Then the reactor was filled with Argon and further heated to 310 °C. After that, 2 mmol of Se and 2 mmol of S dissolved in 2 ml TOP was swiftly injected into the hot mixture, followed by holding the reaction for 10 min. Then, in order to coat an additional ZnS shell, 1.6 mmol of S with 2.4 ml of ODE was injected and the mixture was left to react for 12 min. Then 5 ml Zn(OA)$_2$ was injected and the temperature was controlled to 270 °C. Next, 5 ml of TOP dissolving 9.65 mmol of S was injected into the mixture in a rate of 10 ml/min. And the reaction was maintained at that temperature for 20 min. To purify the synthesized QDs, excess acetone and methanol was added to precipitate the QDs, followed by centrifugation at a speed of 7000 rpm for 10 min. The purified QDs were dispersed in toluene for later use. The 0.1 M CuO solution was prepared by mixing copper acetate, 3 ml of 2-methoxyethanol as the solvent and 150 μl of monoethanolamine as stabilizer.

2.1.2. Device fabrication and characterization

The glass substrates with patterned ITO were cleaned sequentially by sonication in detergent, de-ionized water, acetone and isopropyl alcohol and treated with O$_2$-plasma for 25 min. A thin layer of CuO as HIL was spin-deposited at 4000 rpm for 60 s, followed by baking at different temperatures for 20 min in N$_2$-purged glove box, and the substrates with HIL were treated with UV-ozone for 10 min. PVK (Poly(9-vinylcarbazole)) (10 mg/ml) in chlorobenzene was spin-coated at 3000 rpm for 60 s and thermally annealed at 150 °C for 30 min. The QD layer was formed by depositing 12.5 mg/ml QD in toluene on the ITO/CuO/PVK layer at a speed of 1000 rpm for 60 s and subsequently annealed at 90 °C for 30 min. Then, on top of the QD layer, 2,2′,2″-(1,3,5-Benzinetriyl)-tris(1-phenyl-1-H-benzimidazole) (TPBi), LiF and Al were sequentially thermal-evaporated under a based pressure of ~2.0 × 10^{-4} Pa. The effective area of the LED devices is 4 mm^2.

UPS measurement was performed by using X-ray Photoelectron Spectroscopy (XPS) (VG Escalab 220i XL) with a He I (21.2 eV) gas discharge lamp. AFM (Cypher S, Asylum Research) was used to image the CuO films. XPS data was acquired by a homemade UHV system with monochromatic X-ray source at hv = 1286.7 eV from SPECS and Omircon electron analyzer (EA125). The current density–luminance–voltage (J–L–V) characteristics were measured using a programmable Yogakawa GS610 source measurement unit. The electroluminescence spectra of the QD-LEDs were acquired by a PhotoResearch SpectraScan PR 705 spectrometer. All measurements were carried out at room temperature under ambient conditions.

3. Results and discussion

The CuO solutions prepared as described above were spin-coated onto O$_2$-plasma pre-treated ITO substrates and annealed at different temperatures (90 °C, 120 °C and 150 °C, respectively) for 20 min inside N$_2$-filled glove box. Fig. 1 shows the atomic force microscopy (AFM) images of the CuO films spin-coated from solutions with different annealing temperatures. It can be observed that the surface roughness (RMS) of the films becomes bigger with the increase of the annealing temperatures, specifically it is 1.84 nm for 90 °C, 2.26 nm for 120 °C and 4.58 nm for 150 °C, respectively. The roughness of surface plays an important role in the performance of our QD-LEDs, as we will discuss later in this article.

X-ray photoemission spectroscopy (XPS) was performed to further investigate the surface characteristics of the CuO films. Fig. 2(a) shows a full scan spectrum of the annealed CuO film. The presence of copper and oxygen is evident in the full spectrum with the characteristic peaks at 530.8 eV for O 1 s and 933.4 eV for Cu 2p, respectively. Note that additional strong peaks of In 3d, Sn 3d are originated from the ITO substrate, demonstrating very thin CuO films [23]. Fig. 2(b) shows the XPS spectrum of Cu 2p core level, from which the peaks at 933.4 eV and 953.2 eV correspond to the Cu 2p$_{3/2}$ and Cu 2p$_{1/2}$, respectively [31]. These two peaks indicate that copper is in the II oxidation state. Besides, the two satellite peaks at 961.4 eV and 941.5 eV further demonstrate the oxide in the sample as CuO compound [32,33].

The CuO-based QD-LEDs have a multilayer structure of ITO/CuO/PVK/CdSe@ZnS core–shell structured QDs/TPBi/LiF/Al as depicted in Fig. 3(a). Here CuO is used to replace PEDOT:PSS, which is a common material for the hole injection in organic electronic devices. Meanwhile, PVK and TPBi with respective thicknesses of about 20 nm and 35 nm were chosen as the hole transport layer (HTL) and electron transport layer (ETL) respectively. Fig. 3(b) presents the energy band diagram of the QD-LED studied, where the valence band energy level of CuO films was obtained by our own measurement while those of other components were taken from literatures [27,34–36]. Ultraviolet photoelectron spectroscopy (UPS) measurement was applied to identify the electronic structure of CuO film. The resulting full-scan spectrum, secondary-electron cut-off and valence-band regions of CuO are shown in Fig. 3(c–e), respectively. The valence band maximum (VBM) was estimated to be 5.48 eV by using the incident photon energy (21.2 eV), the high-binding energy cutoff (E_{cutoff}) (Fig. 3(d)), and the onset energy in valance-band region (E_{onset}) (Fig. 3(e)) according to the equation of VBM = 21.2 − (E_{cutoff} − E_{onset}). According to the energy band diagram, electrons are injected from the LUMO level of TPBi into the conduction band of QDs spontaneously while holes are transported from the VBM of CuO and HOMO level of PVK to the valence band of QDs, following by the radiative recombination inside the active layer of QDs.
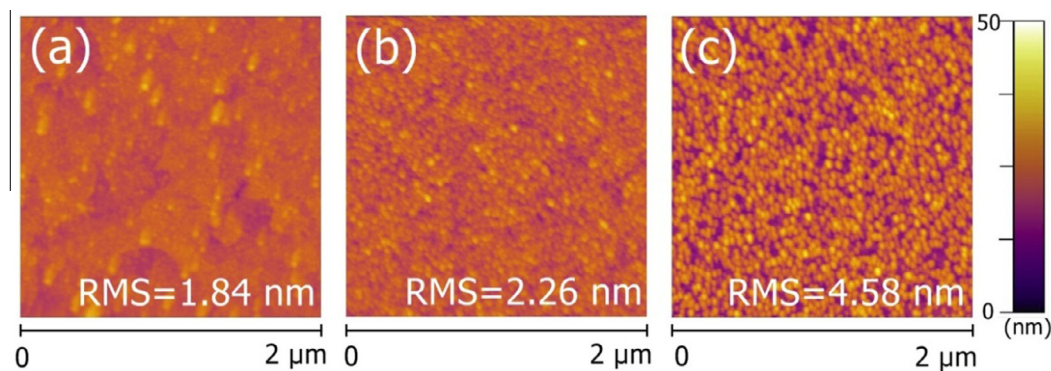
Fig. 1. AFM height images of CuO thin films annealed at (a) 90 °C, (b) 120 °C and (c) 150 °C, respectively.
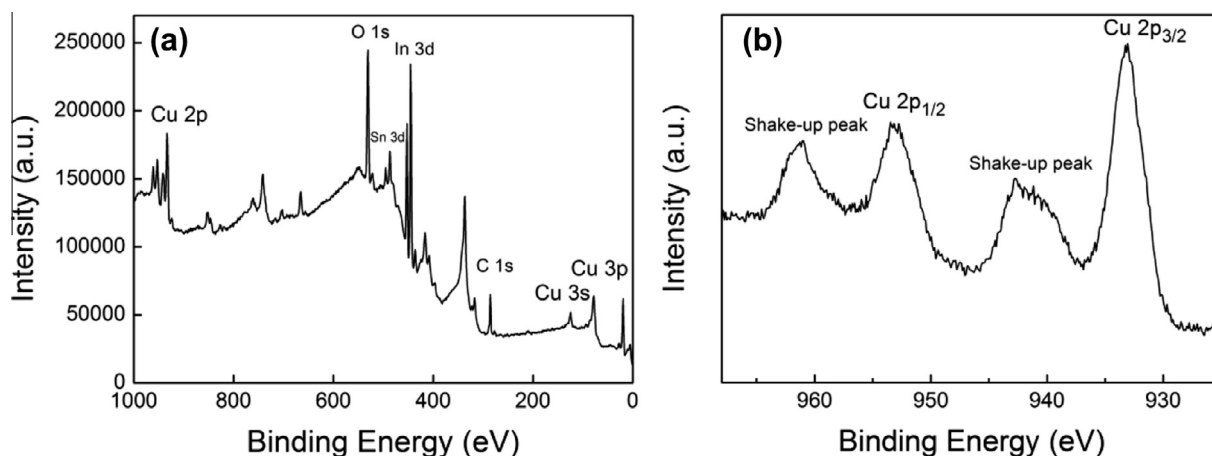

Fig. 2. Photoemission (XPS) spectra of solution-processed CuO film: (a) Wide scan spectrum; (b) high-resolution XPS scan for Cu 2p core level.

Table 1 gives the detailed parameters of QD-LEDs using CuO hole injection layers from the solutions of different annealing temperatures. The device with CuO HIL under 120 °C annealing temperature shows the best EQE of 5.37% with a current efficiency of 21.3 cd/A. Fig. 4(a) shows the spectrum of the normalized QD-LED electroluminescence (EL). The EL spectrum demonstrates a characteristic emission peak with a center wavelength of 522 nm and a FWHM around 20 nm. The current density–voltage–luminance (J–V–L) characteristics of the QD-LED with an annealing temperature of 120 °C is presented in Fig. 4(b), giving a peak luminance of 78,830 cd/m^2 at the current density of 1035 mA/cm^2. The EL curve shows only the pure QD EL emission at the wavelength of 522 nm without the common weak emission in the blue region originated from PVK. This electroluminance spectrum indicates a balanced charge injection from both sides: the electrons injected from TPBi recombine well with the holes from CuO film and PVK side although the energy barriers for these two carriers are different, which, from another point of view, demonstrates an excellent p-type injection capacity for the metal oxide-based thin films. In order to discuss the difference of the performance of the devices acquired under different annealing temperatures, hole-only devices (ITO/CuO/PVK (~100 nm)/MoO$_3$ (40 nm)/Al) were fabricated. Fig. 5(a) shows the current density–voltage characteristics of CuO films with different annealing temperatures. And the influences of annealing temperatures on the workfunction (WF) of CuO films are shown in Fig. 5(b), giving WF values of 5.15 eV, 5.20 eV and 5.21 eV for films annealed at 90 °C, 120 °C and 150 °C, respectively according to the equation of WF = 21.2 − E$_{cutoff}$. It has been well recognized that the increase

of workfunction of hole injection material can enhance the hole injection in organic electroluminescent devices due to the reduced energy barrier [37]. Here, such improved hole injection resulted from the enhanced WF is further demonstrated by the J–V characteristics of the hole-only devices with different annealing temperatures, as shown in Fig. 5(a). Therefore the differences of the device performance can be explained by the comprehensive consideration of the following factors: the surface roughness, the workfunction and the influenced J–V characteristics of hole-only devices. The smaller workfunction of 90 °C annealed film with the resulted inferior hole-injection capability under 90 °C annealing leads to the reduced device performance; On the other hand, QD-LEDs with 120 °C and 150 °C annealing show comparable workfunctions and similar J–V characteristics while the device with 150 °C annealing exhibits some fluctuation at high applied voltages, which can be related to the higher surface roughness of 150 °C annealed CuO film. Similar effects have been observed previously in other structures [38]. Therefore, taking the abovementioned factors together, the device with CuO films annealed at 120 °C presents the best performance.

To further confirm the usefulness of CuO film in QD-LED, a device without using CuO film was compared with a configuration of ITO/PVK/QDs/TPBi/LiF/Al. Fig. 6(a) shows the current density–voltage–luminance comparison of the devices with and without CuO as hole injection layer, respectively. The device without CuO film as hole injection layer presents a peak current density of 37.9 mA/cm^2 and maximum luminance of 6397 cd/m^2, which exhibits much worse performance compared with CuO-based device. This result suggests that the thin CuO layer can significantly
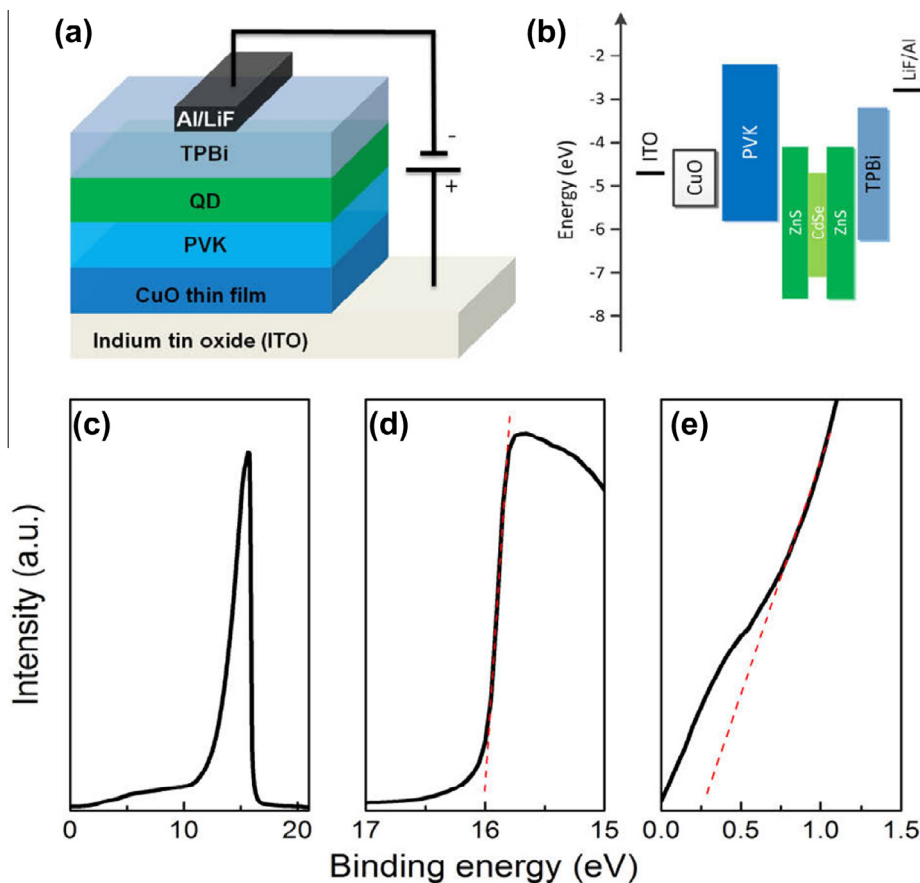
Fig. 3. (a) Schematic structure of the CuO-based QD-LED. (b) Flat-band energy level diagram of QD-LED. UPS spectra showing (c) full-scan spectrum, (d) high-binding energy secondary-electron cutoff regions and (e) valence-band edge regions of CuO films annealed at 120 °C.

Table 1
Detailed parameters of device performance using CuO HTL with different annealing temperatures.

Annealing temperature (°C)	Max. current density (mA/cm^2)	Max. luminance (cd/m^2)	Max. EQE (%)	Max. current efficiency (CE) (cd/A)	Max. power efficiency (PE) (lm/W)
90	725.5	44,650	2.74	10.03	2.29
120	1035.0	78,830	5.37	21.3	7.25
150	704.0	63,890	4.19	14.3	3.16

enhance the hole injection at the interface between the ITO substrate and the active layer. We further compared the CuO-based device with a typical PEDOT:PSS-based QD-LED, where the device structure and various layer thicknesses are exactly the same except the PEDOT:PSS layer thickness is optimized. Fig. 6(b) compares the current density–voltage–luminance characteristics of the CuO and PEDOT:PSS-based QD-LEDs. It can be seen that the CuO-based QD-LED demonstrates both a higher current density and a higher luminance compared to the PEDOT:PSS-based QD-LED. Table 2 tabulates the key parameters of these two QD-LEDs for easy comparison. Much higher maximum brightness and power efficiency are
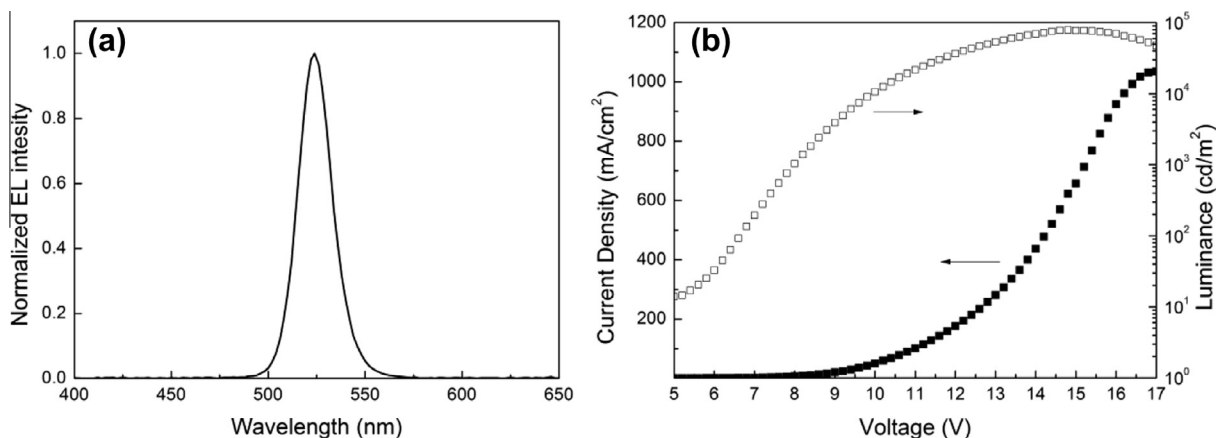

Fig. 4. (a) EL spectrum and (b) current density–voltage–luminance (*J*–*V*–*L*) characteristics of QD-LED.
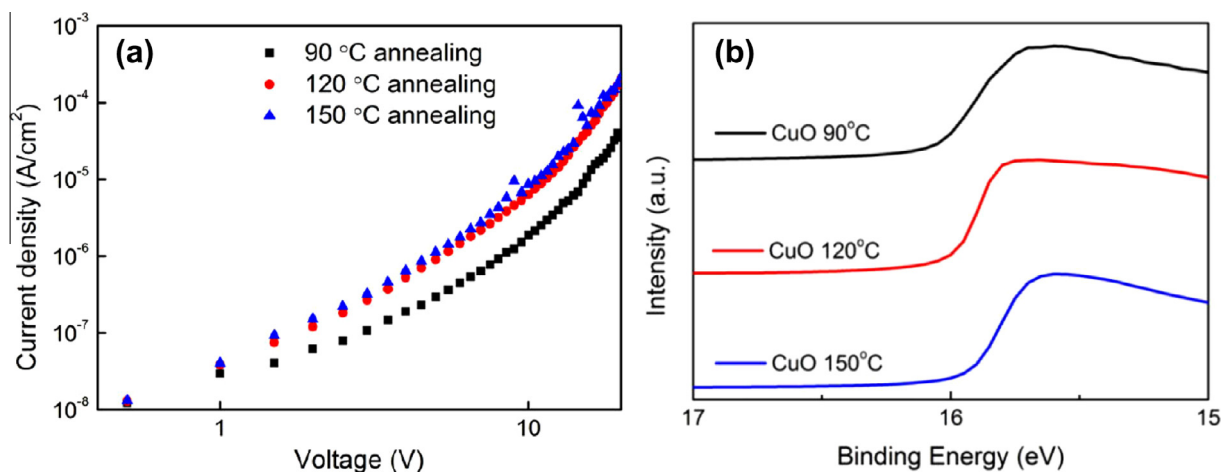
Fig. 5. (a) Current density–voltage characteristics of hole-only device based on CuO films with different annealing temperatures. (b) Secondary-electron cutoff region of CuO films with different annealing temperatures.
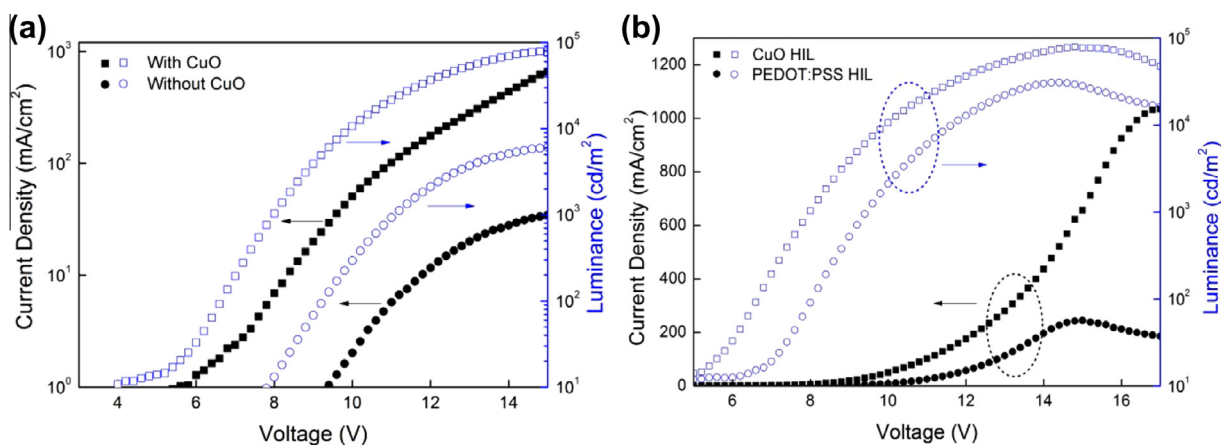

Fig. 6. (a) Current density–voltage–luminance (J–V–L) characteristics of devices with CuO and without CuO film as charge injection layers. (b) Comparison of the current density–voltage–luminance (J–V–L) characteristics of the CuO-based and PEDOT:PSS-based QD-LEDs.

Table 2
Comparison of parameters of device performance using CuO thin film and PEDOT:PSS as HILs, respectively.

Type of HIL	Max. luminance (cd/m^2)	Max. current density (mA/cm^2)	Max. EQE (%)	Max. CE (cd/A)	Max. PE (lm/W)
CuO	78,830	1035.0	5.37	21.3	7.25
PEDOT:PSS	30,870	244.9	5.72	22.9	6.09

acquired by the CuO-based QD-LEDs, and the rest parameters are similar for both devices. To evaluate the stability of QD-LEDs, the operating lifetime measurements were tested under constant driving currents with an initial luminance of 1000 cd/m^2 for both devices. As can be seen in Fig. 7, a better device stability was achieved for CuO-based device when compared with PEDOT:PSS-based one. Thus, CuO can be used as an effective alternative hole injection layer replacing PEDOT:PSS for QD-LED.

4. Conclusion

In conclusion, high-performance copper oxide-based QD-LEDs have been demonstrated and characterized. The preparation of the CuO film was obtained by a simple solution process, yet showing a superior hole injection capability. The optimized CuO-based
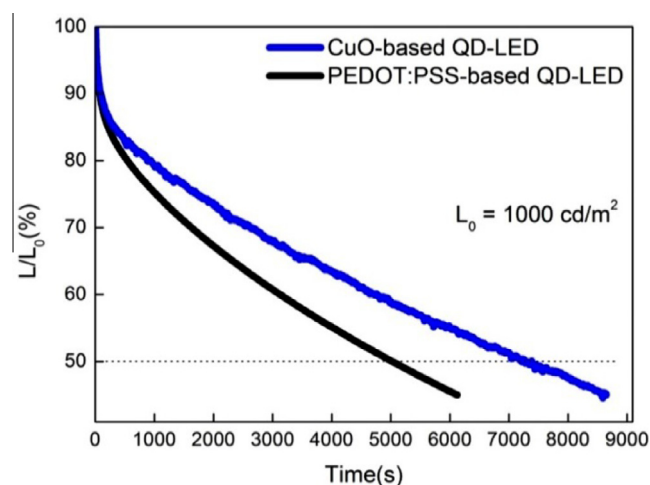

Fig. 7. Lifetime characteristics of CuO-based and PEDOT:PSS-based QD-LED. The measurements were taken without encapsulation and under constant driving currents corresponding to an initial luminance of 1000 cd/m^2 for both devices.

QD-LED presents a high EQE of 5.37% with a maximum luminance over 70,000 cd/m^2. Besides, the overall performance such as the

brightness, EQE and current efficiency are all better or at least comparable to the PEDOT:PSS-based QD-LED using the same structure. These results validate CuO as an alternative solution-processed hole injection materials replacing PEDOT:PSS.

Acknowledgements

References

[1] Y. Shirasaki, G.J. Supran, M.G. Bawendi, V. Bulovic, Emergence of colloidal quantum-dot light-emitting technologies, Nat. Photon. 7 (2013) 13–23.
[2] L. Qian, Y. Zheng, J. Xue, P.H. Holloway, Stable and efficient quantum-dot light-emitting diodes based on solution-processed multilayer structures, Nat. Photon. 5 (2011) 543–548.
[3] J. Kwak, W.K. Bae, D. Lee, I. Park, J. Lim, M. Park, H. Cho, H. Woo, D.Y. Yoon, K. Char, Bright and efficient full-color colloidal quantum dot light-emitting diodes using an inverted device structure, Nano Lett. 12 (2012) 2362–2366.
[4] K.W. Song, R. Costi, V. Bulovic, Electrophoretic deposition of CdSe/ZnS quantum dots for light-emitting devices, Adv. Mater. 25 (2013) 1420–1423.
[5] J.W. Stouwdam, R.A. Janssen, Red, green, and blue quantum dot LEDs with solution processable ZnO nanocrystal electron injection layers, J. Mater. Chem. 18 (2008) 1889–1894.
[6] V. Colvin, M. Schlamp, A. Alivisatos, Light-emitting diodes made from cadmium selenide nanocrystals and a semiconducting polymer, Nature 370 (1994) 354–357.
[7] L. Kim, P.O. Anikeeva, S.A. Coe-Sullivan, J.S. Steckel, M.G. Bawendi, V. Bulovic, Contact printing of quantum dot light-emitting devices, Nano Lett. 8 (2008) 4513–4517.
[8] T. Zhu, K. Shanmugasundaram, S. Price, J. Ruzyllo, F. Zhang, J. Xu, S. Mohney, Q. Zhang, A. Wang, Mist fabrication of light emitting diodes with colloidal nanocrystal quantum dots, Appl. Phys. Lett. 92 (2008) 023111.
[9] V. Wood, M. Panzer, J. Halpert, J.-M. Caruge, M. Bawendi, V. Bulovic, Selection of metal oxide charge transport layers for colloidal quantum dot LEDs, ACS Nano 3 (2009) 3581–3586.
[10] W.K. Bae, J. Kwak, J. Lim, D. Lee, M.K. Nam, K. Char, C. Lee, S. Lee, Multicolored light-emitting diodes based on all-quantum-dot multilayer films using layer-by-layer assembly method, Nano Lett. 10 (2010) 2368–2373.
[11] J.-M. Caruge, J.E. Halpert, V. Bulovic, M.G. Bawendi, NiO as an inorganic hole-transporting layer in quantum-dot light-emitting devices, Nano Lett. 6 (2006) 2991–2994.
[12] J. Zhao, J.A. Bardecker, A.M. Munro, M.S. Liu, Y. Niu, I.-K. Ding, J. Luo, B. Chen, A.K.-Y. Jen, D.S. Ginger, Efficient CdSe/CdS quantum dot light-emitting diodes using a thermally polymerized hole transport layer, Nano Lett. 6 (2006) 463–467.
[13] J. Caruge, J. Halpert, V. Wood, V. Bulović, M. Bawendi, Colloidal quantum-dot light-emitting diodes with metal-oxide charge transport layers, Nat. Photon. 2 (2008) 247–250.
[14] P.O. Anikeeva, J.E. Halpert, M.G. Bawendi, V. Bulovic, Electroluminescence from a mixed red-green-blue colloidal quantum dot monolayer, Nano Lett. 7 (2007) 2196–2200.
[15] M. Schlamp, X. Peng, A. Alivisatos, Improved efficiencies in light emitting diodes made with CdSe (CdS) core/shell type nanocrystals and a semiconducting polymer, J. Appl. Phys. 82 (1997) 5837–5842.
[16] J.J. Li, Y.A. Wang, W. Guo, J.C. Keay, T.D. Mishima, M.B. Johnson, X. Peng, Large-scale synthesis of nearly monodisperse CdSe/CdS core/shell nanocrystals using air-stable reagents via successive ion layer adsorption and reaction, J. Am. Chem. Soc. 125 (2003) 12567–12575.
[17] Q. Sun, Y.A. Wang, L.S. Li, D. Wang, T. Zhu, J. Xu, C. Yang, Y. Li, Bright, multicoloured light-emitting diodes based on quantum dots, Nat. Photon. 1 (2007) 717–722.
[18] X. Dai, Z. Zhang, Y. Jin, Y. Niu, H. Cao, X. Liang, L. Chen, J. Wang, X. Peng, Solution-processed, high-performance light-emitting diodes based on quantum dots, Nature 515 (2014) 96–99.
[19] B.S. Mashford, M. Stevenson, Z. Popovic, C. Hamilton, Z.Q. Zhou, C. Breen, J. Steckel, V. Bulovic, M. Bawendi, S. Coe-Sullivan, P.T. Kazlas, High-efficiency quantum-dot light-emitting devices with enhanced charge injection, Nat. Photon. 7 (2013) 407–412.
[20] K.-H. Lee, J.-H. Lee, W.-S. Song, H. Ko, C. Lee, J.-H. Lee, H. Yang, Highly efficient, color-pure, color-stable blue quantum dot light-emitting devices, ACS Nano 7 (2013) 7295–7302.
[21] M.-Y. Lin, C.-Y. Lee, S.-C. Shiu, I.-J. Wang, J.-Y. Sun, W.-H. Wu, Y.-H. Lin, J.-S. Huang, C.-F. Lin, Sol–gel processed CuOx thin film as an anode interlayer for inverted polymer solar cells, Org. Electron. 11 (2010) 1828–1834.
[22] M.T. Greiner, M.G. Helander, W.-M. Tang, Z.-B. Wang, J. Qiu, Z.-H. Lu, Universal energy-level alignment of molecules on metal oxides, Nat. Mater. 11 (2012) 76–81.
[23] S. Murase, Y. Yang, Solution processed MoO₃ interfacial layer for organic photovoltaics prepared by a facile synthesis method, Adv. Mater. 24 (2012) 2459–2462.
[24] Z. Tan, L. Li, C. Cui, Y. Ding, Q. Xu, S. Li, D. Qian, Y. Li, Solution-processed tungsten oxide as an effective anode buffer layer for high-performance polymer solar cells, J. Phys. Chem. C 116 (2012) 18626–18632.
[25] Z. Tan, L. Li, F. Wang, Q. Xu, S. Li, G. Sun, X. Tu, X. Hou, J. Hou, Y. Li, Solution-processed rhenium oxide: a versatile anode buffer layer for high performance polymer solar cells with enhanced light harvest, Adv. Energy Mater. 4 (2014) 1–7.
[26] X. Yang, Y. Ma, E. Mutlugun, Y. Zhao, K.S. Leck, S.T. Tan, H.V. Demir, Q. Zhang, H. Du, X.W. Sun, Stable, efficient, and all-solution-processed quantum dot light-emitting diodes with double-sided metal oxide nanoparticle charge transport layers, ACS Appl. Mater. Interfaces 6 (2013) 495–499.
[27] X. Yang, E. Mutlugun, Y. Zhao, Y. Gao, K.S. Leck, Y. Ma, L. Ke, S.T. Tan, H.V. Demir, X.W. Sun, Solution processed tungsten oxide interfacial layer for efficient hole-injection in quantum dot light-emitting diodes, Small 10 (2014) 247–252.
[28] Y. Liu, L. Liao, J. Li, C. Pan, From copper nanocrystalline to CuO nanoneedle array: synthesis, growth mechanism, and properties, J. Phys. Chem. C 111 (2007) 5050–5056.
[29] Y.S. Lee, D. Chua, R.E. Brandt, S.C. Siah, J.V. Li, J.P. Mailoa, S.W. Lee, R.G. Gordon, T. Buonassisi, atomic layer deposited gallium oxide buffer layer enables 1.2 V open-circuit voltage in cuprous oxide solar cells, Adv. Mater. 26 (2014) 4704–4710.
[30] K.H. Lee, J.H. Lee, H.D. Kang, B. Park, Y. Kwon, H. Ko, C. Lee, J. Lee, H. Yang, Over 40 cd/A efficient green quantum dot electroluminescent device comprising uniquely large-sized quantum dots, ACS Nano 8 (2014) 4893–4901.
[31] C.-K. Wu, M. Yin, S. O'Brien, J.T. Koberstein, Quantitative analysis of copper oxide nanoparticle composition and structure by X-ray photoelectron spectroscopy, Chem. Mater. 18 (2006) 6054–6058.
[32] C. Huo, J. Ouyang, H. Yang, CuO nanoparticles encapsulated inside Al-MCM-41 mesoporous materials via direct synthetic route, Sci. Rep. 4 (2014) 3682.
[33] M. Yin, C.-K. Wu, Y. Lou, C. Burda, J.T. Koberstein, Y. Zhu, S. O'Brien, Copper oxide nanocrystals, J. Am. Chem. Soc. 127 (2005) 9506–9511.
[34] X.Y. Yang, Y. Divayana, D.W. Zhao, K.S. Leck, F. Lu, S.T. Tan, A.P. Abiyasa, Y.B. Zhao, H.V. Demir, X.W. Sun, A bright cadmium-free, hybrid organic/quantum dot white light-emitting diode, Appl. Phys. Lett. 101 (2012) 233110.
[35] K.S. Leck, Y. Divayana, D. Zhao, X. Yang, A.P. Abiyasa, E. Mutlugun, Y. Gao, S. Liu, S.T. Tan, X.W. Sun, Quantum dot light-emitting diode with quantum dots inside the hole transporting layers, ACS Appl. Mater. Interfaces 5 (2013) 6535–6540.
[36] T. Oku, R. Motoyoshi, K. Fujimoto, T. Akiyama, B. Jeyadevan, J. Cuya, Structures and photovoltaic properties of copper oxides/fullerene solar cells, J. Phys. Chem. Solids 72 (2011) 1206–1211.
[37] A. Baba, K. Onishi, W. Knoll, R.C. Advincula, Investigating work function tunable hole-injection/transport layers of electrodeposited polycarbazole network thin films, J. Phys. Chem. B 108 (2004) 18949–18955.
[38] M. Prietsch, R. Ludeke, Ballistic-electron-emission microscopy and spectroscopy of GaP (110)-metal interfaces, Phys. Rev. Lett. 66 (1991) 2511.